

Diffusive Migration of Low-Mass Proto-planets in Turbulent Disks

Eric T. Johnson and Jeremy Goodman

Department of Astrophysical Sciences, Princeton University, Princeton, NJ 08544

and

Kristen Menou

Department of Astronomy, Columbia University, 550 W. 120th St., New York, NY 10027

ABSTRACT

Torque fluctuations due to magnetorotational turbulence in proto-planetary disks may greatly influence the migration patterns and survival probabilities of nascent planets. Provided that the turbulence is a stationary stochastic process with finite amplitude and correlation time, the resulting diffusive migration can be described with a Fokker-Planck equation, which we reduce to an advection-diffusion equation. We calibrate the coefficients with existing turbulent-disk simulations and mean-migration estimates, and solve the equation both analytically and numerically. Diffusion tends to dominate over advection for planets of low-mass and those in the outer regions of proto-planetary disks, whether they are described by the Minimum Mass Solar Nebula (MMSN) or by T-Tauri alpha disks. Diffusion systematically reduces the lifetime of most planets, yet it allows a declining fraction of them to survive for extended periods of time at large radii. Mean planet lifetimes can even be formally infinite (e.g. in an infinite steady MMSN), though median lifetimes are always finite. Surviving planets may linger near specific radii where the combined effects of advection and diffusion are minimized, or at large radii, depending on model specifics. The stochastic nature of migration in turbulent disks challenges deterministic planet formation scenarios and suggests instead that a wide variety of planetary outcomes are possible from similar initial conditions. This would contribute to the diversity of (extrasolar) planetary systems.

Subject headings: accretion, accretion disks — planetary systems: formation — planetary systems: proto-planetary disks

1. Introduction

A decade of extrasolar planet discoveries has shown that the process of planet formation is more complex than originally anticipated. It leads to a remarkable diversity of planetary configurations, ranging from migrating hot Jupiters to eccentric giant planets, as well as our own “circular” Solar

System. Following these discoveries, progress has been made in understanding planet formation, but the theory is still incomplete (e.g. Marcy et al. 2000; Wuchterl et al. 2000; Papaloizou & Terquem 2006; Armitage & Rice 2006).

The leading scenario for the formation of giant planets is the core accretion mechanism. Icy planetesimals located beyond the snow line in their host disk collide repeatedly to grow a core with a modest gaseous atmosphere. If this core succeeds in reaching a critical mass of a few tens of Earth masses, runaway accretion of a massive gaseous envelope proceeds and leads, ultimately, to the formation of a gaseous giant planet (Safronov 1969; Mizuno 1980; Pollack et al. 1996). Some evidence supporting this scenario has emerged in recent years, in the form of a metallicity trend for stars hosting planets (e.g. Santos et al. 2004; Gilliland et al. 2000; Weldrake et al. 2005), the discovery of a high density hot Jupiter (Sato et al. 2005) and that of a surprisingly low-mass microlensing planet (Beaulieu et al. 2006). However, a long-standing difficulty for the core accretion scenario, which has not yet been fully elucidated, is the fact that the timescale required to build-up critical core masses and thus large gaseous envelopes ($\sim 10^6$ - 10^7 yr) is comparable to the lifetimes of proto-planetary disks (e.g. Pollack et al. 1996; Papaloizou & Terquem 1999).

Orbital migration adds a layer of complication to theories of planet formation. As a result of gravitational interactions with their gaseous disk (Goldreich & Tremaine 1980; Lin & Papaloizou 1986), the orbits of planets in the terrestrial mass range are predicted to decay on timescales ($\sim 10^5$ yr) short compared to disk lifetimes (e.g. Korycansky & Pollack 1993; Ward 1997a,b). Migration is slower for planets of much smaller or much larger masses: in the first case because the torque causing migration is quadratic in planet mass, and in the second case because the planet opens a gap and then migrates on the disk's accretion timescale, which can be comparable to its lifetime. While it is possible or probable that many terrestrial planets form by agglomeration of smaller bodies after the gas is gone, this is not an option for the solid cores of Jovian planets since, in the core accretion scenario, the cores must form before the gaseous envelopes can be accreted. The prevalence of Jovian planets with orbital periods of only a few days deepens the mystery as it suggests that these planets did migrate but stopped short of merging with their stars at orbital radii where even the accretion timescale would seem to have been very short (e.g. Lin et al. 1996).

Analytic calculations and most hydro-dynamical simulations of migration usually assume a disk that is laminar apart from the waves and shocks excited by the planet itself (e.g. Korycansky & Pollack 1993; Ward 1997a; Kley et al. 2001; Nelson & Benz 2003a,b; D'Angelo et al. 2003; Lufkin et al. 2004; Schaefer et al. 2004). But the effective viscosity of disks probably involves turbulence. Nelson & Papaloizou (2004), Laughlin et al. (2004), and Nelson (2005, hereafter N2005) have found in 3D simulations of magneto-rotational turbulence that the instantaneous torque exerted on a planet in the terrestrial mass range is subject to fluctuations many times its mean value, apparently caused by turbulent density fluctuations in the planet's vicinity. In fact, no obvious secular decay manifests itself in the orbits of planets with mass $M_p \lesssim 10M_\oplus$, although because the simulations are limited to $\sim 10^2$ planetary orbits—compare $\gtrsim 10^5$ for Jupiter during the lifetime of the proto-solar nebula—and the predicted decay in semimajor axis is $\lesssim 10\%$ over this period,

the expected secular trend might be difficult to discern amid the fluctuations.

The possibility that planetary torques are stochastic raises several issues:

1. Is the time-averaged torque exerted on a planet of a given angular momentum affected? N2005 finds that turbulence excites planetary eccentricity, e . In linear theory, eccentricity allows the planet to interact with the disk at additional resonances that do not couple to circular orbits (Goldreich & Tremaine 1980; Goldreich & Sari 2003). Also, at second and higher orders in e , the radial positions of the original resonances shift if one compares eccentric and circular orbits at fixed angular momentum; they do not shift at fixed orbital energy since keplerian energies and mean motions vary only with semi-major axis. Thus for eccentric planets, one must distinguish the rate of change of the planetary angular momentum (torque) from the rate of change of orbital energy. Smoothing of the planetary potential along epicycles tends to reduce the strength of the highest- m Lindblad resonances that dominate the torque on circular orbits. All of these perturbative effects are expected to become significant when $e \gtrsim h/r$, where $h \equiv c_s/\Omega$ is the disk thickness. Planets of terrestrial mass achieved such eccentricities in N2005’s simulations. On the other hand, at about the same eccentricity the epicyclic velocities become supersonic, which will probably raise significant shocks, a non-perturbative effect. Thus both the sign and magnitude of the changes in the mean torque due to turbulently excited eccentricity are unclear. We are not aware of any systematic investigation of this issue, nor have we attempted one. Throughout this paper, we treat the planetary orbit as circular.
2. Even for circular orbits, stochastic changes in semi-major axis on timescales long compared to the period but short compared to the nominal migration time may significantly alter the mean orbital lifetime. This is particularly likely when the local mean torque varies strongly with radius, as it does in the alpha disks studied by Menou & Goodman (2004). Because of rapid changes in opacity in certain temperature regimes, the disks exhibit sharp peaks in the local migration timescale. Under laminar conditions, orbital lifetimes can be dominated by the time required to drift across these peaks. Turbulent fluctuations in the torque, however, could allow planets to “jump over” the peaks, thus shortening the lifetime. On the other hand, diffusion to large radii where the local migration time is long might prolong the orbital lifetime.
3. Finally, orbital diffusion should allow the occasional planet to survive much longer than the mean lifetime defined by its birthplace. If sufficiently many planets are formed, this might in principle help to reconcile theoretical predictions of rapid *mean* migration with the observations at least of the longer-period planets (though it seems unlikely to explain hot Jupiters).

The methods adopted in this paper allow us to explore the second and third issues above, but not the first. In §2, we develop a simple advection-diffusion or Fokker-Planck equation for the

probability distribution function of planetary orbital angular momentum in the presence of torque fluctuations. Parametrizations of the advection and diffusion coefficients are calibrated against semianalytic formalisms and the simulations of N2005, respectively. §3 explores analytic steady-state and time-dependent solutions to this equation in steady disks whose properties are power laws in radius. §4 and §5 present numerical, time-dependent solutions in such a disk (the Minimum Mass Solar Nebula) and in alpha disks with realistic opacities. A summary of our main results and conclusions is given in §6.

2. Advection-diffusion Equation for Planetary Migration

Planets migrate as a result of torques exerted by the disk. Because of turbulence, the torque is a stochastic function with a mean part $\bar{\Gamma}$ and a fluctuating part $\delta\Gamma$. For a given planetary mass (M_p) and a given time-averaged surface density and thickness of the disk [$\bar{\Sigma}(r)$, $\bar{h}(r)$ respectively], the mean torque depends only on the semimajor axis, r_p , of the planetary orbit, which is assumed to be circular. The diffusion equation is most conveniently derived in terms of the orbital angular momentum¹ $J = M_p\sqrt{GM_*r_p}$, rather than r_p , as the spatial independent variable.

The fluctuating part of the torque depends on time as well as J : $\delta\Gamma = \delta\Gamma(t, J)$. By construction, $\overline{\delta\Gamma} = 0$. The fluctuating torque is taken to be a temporally stationary stochastic process with a finite amplitude and correlation time, so that the integral

$$D(J) \equiv \frac{1}{2} \int_{-\infty}^{\infty} \overline{\delta\Gamma(t - \tau/2, J) \delta\Gamma(t + \tau/2, J)} d\tau \quad (1)$$

exists. $D(J)$ will play the role of diffusion coefficient. The correlation time can then be defined by

$$\tau_c \equiv D(J) / \overline{[\delta\Gamma(t, J)]^2}. \quad (2)$$

Temporal stationarity implies that $D(J)$, $\overline{[\delta\Gamma(t, J)]^2}$, and τ_c are independent of t .

The desired advection-diffusion equation derives from a Fokker-Planck equation, and its formal derivation is completely standard (*e.g.* van Kampen 1981), but it is useful to repeat the derivation here in order to emphasize the underlying assumptions and to ask whether they are justified in this case. Two important assumptions have already been introduced: the finiteness of Eqs. (1) & (2).

Let $P(\Delta J | \Delta t, J)$ be the probability that a planet of initial angular momentum J suffers a change ΔJ during time interval Δt . Moments of the change are

$$\overline{(\Delta J)^n} \equiv \int_{-\infty}^{\infty} (\Delta J)^n P(\Delta J | \Delta t, J) d\Delta J. \quad (3)$$

¹Throughout our analysis, we focus on the limit $M_p \ll M_*$, where M_* is the mass of the central star.

Of course, except for $\overline{(\Delta J)^0} = 1$, these depend implicitly on J and Δt .

Next, let $f(t, J)$ be the probability that the planet has angular momentum J at $t > 0$ given some initial condition at $t = 0$. The probability at $t + \Delta t$ is

$$\begin{aligned} f(t + \Delta t, J) &= \int_{-\infty}^{\infty} P(\Delta J | \Delta t, J - \Delta J) f(t, J - \Delta J) d\Delta J \\ &= \int_{-\infty}^{\infty} \sum_{n=0}^{\infty} \frac{(-1)^n}{n!} (\Delta J)^n \frac{\partial^n}{\partial J^n} [P(\Delta J | \Delta t, J) f(t, J)] d\Delta J \\ &= \sum_{n=0}^{\infty} \frac{(-1)^n}{n!} \frac{\partial^n}{\partial J^n} \left\{ \overline{(\Delta J)^n} f(t, J) \right\}. \end{aligned} \quad (4)$$

In the Fokker-Planck approximation, the changes are presumed small compared to J itself but cumulative, so that one can ignore the terms $n > 2$ in the sum above. More will be said about the justification for this below.

Clearly $\overline{(\Delta J)^0} = 1$, $\overline{\Delta J} = \bar{\Gamma}(J)\Delta t$, and

$$\begin{aligned} \overline{(\Delta J)^2} &= \overline{\left[\bar{\Gamma}(J)\Delta t + \int_0^{\Delta t} \delta\Gamma(t') dt' \right]^2} \\ &= \bar{\Gamma}(J)^2 (\Delta t)^2 + \int_0^{\Delta t} dt_m \int_{-2t_m}^{2t_m} d\tau \overline{\delta\Gamma(t_m - \tau/2, J) \delta\Gamma(t_m + \tau/2, J)}. \end{aligned}$$

The next important assumption is that τ_c is short compared to the timescale on which J changes by order itself—let us write t_J for the latter timescale—so that we may take Δt in the range $\tau_c \ll \Delta t \ll t_J$. In that case, the double integral above $\approx 2D(J)\Delta t$. At this point,

$$f(t + \Delta t, J) \approx f(t, J) + \left[-\frac{\partial}{\partial J} (\bar{\Gamma} f) + \frac{\partial^2}{\partial J^2} (Df) \right] \Delta t + O[(\Delta t)^2],$$

where the $O[(\Delta t)^2]$ part includes the $(\bar{\Gamma}\Delta t)^2$ contribution to $\overline{(\Delta J)^2}$. Neglecting these terms on the grounds that $\Delta t \ll t_J$, one has the desired advection-diffusion equation:

$$\begin{aligned} \frac{\partial f}{\partial t} + \frac{\partial F_J}{\partial J} &= 0 \\ F_J &\equiv \bar{\Gamma}(J)f(t, J) - \frac{\partial}{\partial J} \left[D(J)f(t, J) \right]. \end{aligned} \quad (5)$$

An interesting feature of the above result is that if the diffusion coefficient $D(J)$ varies with J , then it influences the *mean* migration rate. That is to say, one can rewrite the flux in Eq. (5) as

$$F_J = \left(\bar{\Gamma} - \frac{\partial D}{\partial J} \right) f - D \frac{\partial f}{\partial J},$$

so that $-\partial D/\partial J$ contributes to the advection term.

2.1. Calibration of the diffusion and advection coefficients

We have tried to abstract a value and scaling for $D(J)$ from the MHD simulations of N2005; the results of Laughlin et al. (2004) were difficult to translate into our framework. Nelson reports that the typical timescale of fluctuations in $\delta\Gamma$ is of order half an orbital period. Hence we take

$$\tau_c \approx \pi \left(\frac{r_p^3}{GM_*} \right)^{1/2} = \frac{\pi(J/M_p)^3}{(GM_*)^2}. \quad (6)$$

A direct estimate of the correlation function of the data suggests, however, that correlations may persist to much longer than an orbital period, and it is conceivable that the integral (1) for $D(J)$ does not even exist (Nelson 2005, private communication). If the correlation time does not exist, then the methods of this paper are inapplicable to migration. Such long-term correlations imply a “memory” in the turbulence, presumably involving persistent structures in addition to the planet of interest: for example, long-lived vortices (e.g. Fromang & Nelson 2005; Johansen & Klahr 2005), or of course other planets. Pending further numerical evidence, we adopt as a working hypothesis that τ_c *does* exist but with uncertain magnitude.

To complete the diffusion coefficient, we require a parametrization of the variance of the fluctuating torque in terms of time-averaged disk properties. This entails some guesswork, as the simulations of N2005 and Nelson & Papaloizou (2004) have explored only a limited range of disk models and planetary radii. A natural scale for the gravitational force exerted on the planet by the local gas is $2\pi G\Sigma M_p$, where Σ is the surface density of the disk. This is the force that the planet would feel if suspended just above the disk. The corresponding natural scale for the torque is $2\pi G\Sigma M_p r_p$. Therefore, we postulate that the variance of the torque fluctuations is

$$\overline{[\delta\Gamma(t, J)]^2} \approx (\mathcal{C}_D \times 2\pi G\Sigma r_p M_p)^2, \quad (7)$$

where \mathcal{C}_D is a dimensionless coefficient depending upon the strength of the turbulence.

Since the parametrization (7) underlies all of our results, it is worth more discussion. The turbulence is accompanied by density perturbations of r.m.s. amplitude $\delta\rho_\lambda$ on scale λ . An individual perturbation of this scale exerts a gravitational force per unit mass $\sim G\delta\rho_\lambda\lambda^3 d^{-2}$ at distance d if $\lambda < h$, and $\sim G\delta\rho_\lambda h\lambda^2 d^{-2}$ if $\lambda > h$. Presuming that the forces from different perturbations add in quadrature, the mean-square force is dominated by the closest such perturbation, at $d \sim \lambda$, since the number of λ -scale perturbations within distance d increases more slowly with d than the mean-square contribution from individual perturbations decreases: $\propto (d/\lambda)^3$ for $d < h$ and $\propto (d/\lambda)^2$ for $d > h$, versus d^{-4} . Thus, the r.m.s. force due to scale λ is $\delta f_\lambda \sim G\delta\rho_\lambda\lambda$ for $\lambda < h$ and $\delta f_\lambda \sim G\delta\rho_\lambda h \sim G\delta\Sigma_\lambda$ for $\lambda > h$. The contributions to $D(J)$ from $\lambda < h$ are probably unimportant

because of the weighting by λ and because smaller scales are likely to have shorter correlation times. If the density power spectrum were as “blue” as white noise, $\delta\rho_\lambda \propto \lambda^{-3/2}$, and if the correlation time $\tau_{c,\lambda} \propto \lambda$, then there would be equal contributions from all scales $< h$, with the result that the total contribution from these scales would be larger than the contribution from $\lambda \gtrsim h$ by a logarithmic factor. In reality, the density power spectrum is surely red, since local magnetorotational (henceforth MRI) simulations find that most of the turbulent magnetic and kinetic energy resides at scales $\gtrsim h$ (Hawley, Gammie, & Balbus 1995; Brandenburg et al. 1995). Thus, the dominant contribution to the force comes from scales $\gtrsim h$. Since $\delta f_\lambda \sim G\delta\Sigma_\lambda$ in this regime, the total r.m.s. force fluctuation is proportional to the total r.m.s. surface-density fluctuation, $\delta\Sigma$.

It remains to discuss how $\delta\rho/\rho$ and hence $\delta\Sigma/\Sigma$ may depend upon the strength of the turbulence. Density fluctuations may arise from fluctuations in gas pressure or in entropy. Local MRI simulations indicate that $\delta\rho/\rho \sim \delta P/P \sim \delta B^2/8\pi\rho c_s^2 \approx 2\alpha$ (Sano et al. 2003), as might be expected from equipartition, since the internal energy per unit mass associated with a density fluctuation is $c_s^2\delta\rho/\rho$. In a statistically steady accretion disk, the local thermal time $\sim (\alpha\Omega)^{-1}$, so if the correlation time of mechanical fluctuations is $\sim \Omega^{-1}$, entropy fluctuations due to dissipation are expected to be at most $\propto \alpha$. Entropy fluctuations may also arise by advection of material in the presence of a background entropy gradient, $\delta S \approx -\delta\mathbf{x} \cdot \nabla S$. The simulations cited above indicate that the turbulent Reynolds stress scales with the magnetic stress so $\delta\mathbf{v} \sim \alpha^{1/2}c_s$, and we assume that the largest displacements have frequencies $\sim \Omega$, so the r.m.s. displacement $\delta\mathbf{x} \sim \alpha^{1/2}h$ in any direction. Vertical and horizontal entropy gradients are likely to have scale lengths $\sim h$ and $\sim r$, respectively, which would seem to make vertical displacements more important. However, the azimuthal force, and hence torque, exerted by a mass element changes only at second order as it is displaced vertically through $\delta z \sim \alpha^{1/2}h \ll h$, so vertical displacements contribute at $O(\alpha)$. Radial displacements contribute at first order, $(\delta\Sigma/\Sigma)_{dS/dr} \sim \alpha^{1/2}h/r$. The vertically uniform disk of N2005 has a radial entropy gradient, since the sound speed is constant but the density is not; however, since N2005 obtains $\langle\alpha\rangle \approx 5 \times 10^{-3}$ (in agreement with previous work), it happens that $\alpha^{1/2} \approx 0.07 = h/r$ in these models, so that we cannot distinguish between $\delta\Sigma/\Sigma \sim \alpha$ and $\delta\Sigma/\Sigma \sim \alpha^{1/2}h/r$.

It would be useful to calculate torque fluctuations in a variety of disk models with varying entropy gradients, thicknesses, and (if possible) strengths of turbulence. Lacking such information, we provisionally assume $\delta\Sigma \sim f(\alpha)\Sigma$, where f is some function (probably linear). This leads to the parametrization (7) if α is a universal constant. As will be seen, diffusion then dominates mean migration, *i.e.* inward drift at the rate predicted for a laminar disk, in the outer parts of plausible disk models. If $\delta\Sigma$ is also proportional to h/r , diffusion becomes even more dominant in the outer parts of a flaring disk.

N2005 reports that the r.m.s. fluctuating torque per unit planetary mass is $1.5 \pm 0.5 \times 10^{-4}$ in code units. In the same units, $2\pi G\Sigma r_p \approx 3.3 \times 10^{-3}$ (Nelson 2005, private communication); the latter is independent of radius because $\Sigma \propto r^{-1}$. Therefore,

$$\mathcal{C}_D = 0.046 \quad (8)$$

is taken as the reference value of the dimensionless factor in equation (7).

Following Eq. (2), the diffusion coefficient $D(J)$ is the product of the correlation time τ_c (6) and the torque variance (7). Both factors are uncertain, but within the framework of this advection-diffusion approach, they combine into a single parameter. We hope that future numerical simulations will refine our estimates of this parameter and, more importantly, test the validity of the scalings (6) and (7).

For comparison, Ward (1997a)’s expression for the mean Lindblad torque density,

$$\left(\frac{d\Gamma}{dr}\right)_{LR} = \text{sign}(r - r_p) \frac{2\mu^2 \bar{\Sigma} r_p^4 \Omega_p^4}{r(1 + 4\xi^2)\kappa^2} m^4 \psi^2, \quad (9)$$

leads to the scaling

$$\bar{\Gamma} \propto \frac{GM_p^2 r_p^3 \bar{\Sigma}}{M_* h^2}. \quad (10)$$

For consistency with our calibration of torque fluctuations, we also calibrate this relation against Nelson’s simulations of laminar disks, in which the type I torque per unit mass is $\simeq 1.5 \times 10^{-6} M_p/M_\oplus$ in code units. The constant of proportionality in Eq. (10) is then $\simeq -4.8$. Using Eq. (10) implies that the mean torque is always negative. This is fine for plausible power-law disks but might be misleading for alpha disks, where the surface density and temperature can be highly structured, allowing in principle for positive (or at least much reduced) $\bar{\Gamma}$ at some radii. Thus when modeling alpha disks we use Eq. (9) directly, as described in Menou & Goodman (2004).

3. Analytic results

Power-law disk models such as the Minimum-Mass Solar Nebula (hereafter MMSN; Hayashi (1981)) allow the advection-diffusion equation to be solved analytically, at least in steady state. Some aspects of time-dependent evolution can also be determined analytically for this class of disk models. Throughout this section, all disk models are considered to be infinite in radius as well as steady. While unrealistic, this is technically convenient, and we are still able to identify results that are likely to be sensitive to the details of the outer boundary conditions: for example, the mean orbital lifetime. For reference, the MMSN model adopted here has mean surface density $\bar{\Sigma} \propto r^{-3/2}$ and aspect ratio $h/r \propto r^{1/4}$.

3.1. Steady state

A steady-state distribution of planets, $f(J)$, satisfies

$$\frac{\partial F_J}{\partial J} = S(J), \quad (11)$$

where the right-hand side is a source term representing the rate of formation of planets at radius r_p with angular momentum $J = M_p \sqrt{GM_* r_p}$. Analytic solutions to Eq. (11) exist when mean torque and the diffusion coefficient are both power-laws in J :

$$\bar{\Gamma}(J) \propto J^\alpha, \quad D(J) \propto J^\beta, \quad (12)$$

and the source term is a Dirac delta function

$$S(J) = \delta(J - J_S) J_S \Lambda, \quad (13)$$

where Λ is the rate of planet formation at J_S . We see immediately that the flux of planets interior (F_J^-) and exterior (F_J^+) to the source are both constant and related to each other by

$$F_J^+ - F_J^- = J_S \Lambda. \quad (14)$$

First we consider the limiting behavior as $J \rightarrow \infty$. The local timescale for secular inward migration is given by $t_{\text{mig}} = J/|\bar{\Gamma}(J)|$, and the local diffusion timescale is given by $t_{\text{diff}} = J^2/D(J)$. The ratio, $t_{\text{diff}}/t_{\text{mig}} \propto J^{\alpha-\beta+1}$ indicates that the mean torque becomes asymptotically negligible if $\alpha - \beta + 1 < 0$. (This condition holds for the minimum-mass solar nebula, in which $\bar{\Gamma} \propto -J^{-2}$ and $D \propto J$.) For such disks the solution to Eq. (11) at large J exterior to the source becomes $f(J) \approx (\mathcal{C} - J F_J^+)/D(J)$, where \mathcal{C} is a constant of integration. We insist that $F_J^+ \geq 0$ since there should not be an incoming flux of planets from infinity. Thus the numerator eventually becomes negative. The diffusion coefficient $D(J)$ is unquestionably positive, so f becomes negative at sufficiently large J . But this is absurd, since $f(J)dJ$ is a probability. Thus we cannot have both a positive flux and a positive f at large J in steady-state, and it follows that $F_J^+ = 0$ and $F_J^- = -J_S \Lambda$. All the flux generated at the source is accreted through the inner edge of the disk.

We now discuss Eq. (11) in full, emphasizing behavior at small and large J . Let

$$\frac{d\mu}{dJ} = -\frac{\bar{\Gamma}(J)}{D(J)}, \quad (15)$$

so that $\exp[\mu(J)]$ is an integrating factor for Eq. (11). Then

$$f^\pm(J) = \frac{1}{D(J)} e^{-\mu(J)} \left[e^{\mu(J_S)} D(J_S) f(J_S) - F_J^\pm \int_{J_S}^J e^{\mu(\bar{J})} d\bar{J} \right]. \quad (16)$$

As before, the upper (lower) sign on f^\pm and F_J^\pm applies to $J > J_S$ ($J < J_S$). When $\bar{\Gamma}(J)$ and $D(J)$ are power laws, f^\pm can be evaluated explicitly, but we will not write it out. Normally the mean torque $\bar{\Gamma} < 0$, so that $d\mu/dJ > 0$. Then we can choose the constant of integration in Eq. (15) so that $\mu \leq 0$ for $J \leq J_S$ and $\mu \geq 0$ for $J \geq J_S$. All disks of interest in this paper are dominated by the mean torque at small radii and by diffusion at large J . Hence $\exp[-\mu(J)]$ becomes large at small J , and so for a well-behaved solution, the contents of the square brackets in Eq. (16) must tend to zero as $J \rightarrow 0$. This defines a relationship between $f(J_S)$ and F_J^- . For $J > J_S$, $e^{\mu(J)} \geq 1$,

so the integral increases at least as fast as $J - J_S$. As before, if the disk is indefinitely extended then we must have $F_J^+ = 0$ to prevent $f^+(J)$ from becoming negative at large J .

The main conclusion of this discussion is that *as long as the mean torque is nonpositive in the outer disk, the flux of planets diffusing to infinite radius vanishes*. We have reached this conclusion by considering steady solutions but will assume that it applies generally.

3.2. Time-dependent evolution

The time-dependent problem is more difficult, but we can determine some general characteristics of the solution by analytic means, most importantly that *the probability of surviving without accretion in an infinite steady disk, though declining monotonically with time, can have a long power law tail*. For the special case of the MMSN, where $D \propto J$ and $\bar{\Gamma} \propto -J^{-2}$, this probability declines only as t^{-1} . The asymptotic form of the solution at late times is self-similar except near $J = 0$ and is described explicitly in dimensionless units by equation (32).

The evolution of a planet created with $J = J_S$ at $t = 0$ can be represented by solving Eq. (5) with a source term $\delta(t)\delta(J - J_S)$. The Laplace transform

$$\hat{f}(s, J) \equiv \int_0^\infty e^{-st} f(t, J) dt, \quad (17)$$

reduces the time-dependent problem to

$$\frac{\partial^2}{\partial J^2} \left[D(J) \hat{f}(s, J) \right] - \frac{\partial}{\partial J} \left[\bar{\Gamma}(J) \hat{f}(s, J) \right] - s \hat{f}(s, J) = -\delta(J - J_S). \quad (18)$$

Unfortunately, although Eq. (18) is just an ordinary differential equation in J , we cannot solve it completely even for power law disks described by Eq. (12). The difficulty is in part that physically interesting cases have $\alpha - \beta < -1$, which is precisely the condition for Eq. (18) to have an irregular singular point at $J = 0$. However, a formal solution can be obtained in powers of s ,

$$\hat{f}(s, J) = \sum_{n=0}^\infty \frac{(-s)^n}{n!} f_n(J). \quad (19)$$

Replacing $\exp(-st)$ by its Taylor series in the Laplace transform (17) shows that $f_n(J)$ is the n^{th} moment of $f(t, J)$ with respect to t ,

$$f_n(J) = \int_0^\infty t^n f(t, J) dt. \quad (20)$$

More interesting than the moments of f are the moments of the corresponding flux:

$$F_n(J) \equiv -(Df_n)' + \bar{\Gamma}f_n = \int_0^\infty t^n F_J(t, J) dt. \quad (21)$$

The probability that the planet survives longer than t before accretion, $P(t)$, is related to the flux at the origin by $dP/dt = F_J(t, 0)$. Therefore,

$$-F_n(0) = - \int_0^\infty t^n \frac{dP}{dt} dt \quad (22)$$

is the n^{th} moment of the lifetime, and in particular, $-F_1(0)$ is the mean lifetime.

Thus we are motivated to find the $f_n(J)$. Substituting Eq. (19) into Eq. (18) leads to

$$[D(J)f_0(J)]'' - [\bar{\Gamma}(J)f_0(J)]' = -\delta(J - J_S), \quad (23)$$

$$[D(J)f_n(J)]'' - [\bar{\Gamma}(J)f_n(J)]' = -nf_{n-1}(J) \quad n > 0, \quad (24)$$

where the primes indicate derivatives with respect to J . The solution to Eq. (23), which is formally identical to the steady-state case (11), is a Green's function for eq. (24). It can be constructed from homogeneous solutions $y_0(J)$ and $y_1(J)$ with fluxes 0 and -1 , respectively:

$$[D(J)y_0(J)]' - \bar{\Gamma}(J)y_0(J) = 0, \quad (25)$$

$$[D(J)y_1(J)]' - \bar{\Gamma}(J)y_1(J) = 1. \quad (26)$$

The Green's function is

$$G(J, J_S) = y_1(J_<)y_0(J_>)/y_0(J_S), \quad J_< \equiv \min(J, J_S), \quad J_> \equiv \max(J, J_S). \quad (27)$$

The formal solution to the system (23)-(24) is then

$$\begin{aligned} f_0(J) &= G(J, J_S), \\ f_n(J) &= n! \int_0^\infty dJ_1 \dots \int_0^\infty dJ_n G(J, J_1)G(J_1, J_2) \dots G(J_n, J_S). \end{aligned} \quad (28)$$

The existence of the moments (20) therefore depends upon the convergence of the integrals in (28).

An important special case is the MMSN, where $D(J) = D_0J$ and $\bar{\Gamma} = -\Gamma_0J^{-2}$. It is convenient to choose $J_* \equiv (\Gamma_0/D_0)^{1/2}$ as the unit of angular momentum and $t_* \equiv J_*/D_0$ as the unit of time so that $D(J) \rightarrow J$ and $\bar{\Gamma}(J) \rightarrow -J^{-2}$. The homogeneous solutions (25) become

$$y_0(J) = J^{-1}e^{x^2} \quad \text{where } x \equiv \frac{1}{J\sqrt{2}}, \quad (29)$$

$$\begin{aligned} y_1(J) &= 1 - \pi^{1/2}xe^{-x^2}\text{erfc}(x) \\ &\approx \begin{cases} J^2 - (3!!)J^4 + (5!!)J^6 - \dots & J \rightarrow 0^+ \\ 1 - \sqrt{\frac{\pi}{2}} \sum_{n=0}^{\infty} \frac{1}{(2n)!!} J^{-2n-1} + \sum_{n=1}^{\infty} \frac{1}{(2n-1)!!} J^{-2n} & J \rightarrow \infty. \end{cases} \end{aligned} \quad (30)$$

The first expansion is only asymptotic, in keeping with the fact that $J = 0$ is an irregular singular point of Eq. (26), whereas the second converges for all $J \neq 0$.

Armed with these results, we can now determine the convergence of the integrals (28). Because $y_0(J) \propto J^{-1}$ as $J \rightarrow \infty$, it follows from (27) that the integrand for $f_1(J)$ is proportional to J_1^{-1} as $J_1 \rightarrow \infty$. Thus the integral over J_1 is logarithmically divergent. Consequently *the mean lifetime defined by Eq. (22) is not finite*. Since the divergence is only logarithmic, one may guess (correctly) that $P(t) \propto t^{-1}$ at late times in the infinite MMSN.

The long tail in the distribution of lifetimes results from diffusion to large radii where torques are weak and planets linger. It is natural to seek a self-similar solution to Eq. (5) that reflects this behavior. Unfortunately J_* defines a preferred scale that prevents self-similarity. Omitting $\bar{\Gamma}$ from Eq. (5) on the grounds that this term is unimportant at $J \gg J_*$ removes the obstruction:

$$\frac{\partial \tilde{f}}{\partial t}(t, J) = \frac{\partial^2}{\partial J^2}[J\tilde{f}(t, J)], \quad (31)$$

in the present dimensionless units with $D(J) \propto J$ as in the MMSN. The tilde distinguishes the solution to the approximate equation (31) from the exact solution $f(t, J)$ of Eq. (5). We require $\tilde{f} \rightarrow 0$ as $J \rightarrow \infty$. On the other hand, $\tilde{f}(t, J)$ should be positive and finite at $J = 0$ for the following reason. At late times such that $J \ll \sqrt{D(J)t}$, we expect $f(t, J)$ to match onto a multiple of the constant-flux steady-state solution defined by Eq. (30): $f(t, J) \approx -F_J(t, 0)y_1(J)$. We may replace f with \tilde{f} in this relation if $J \gg J_*$, and in that region $y_1(J) \approx 1$. Eq. (31) can be solved with these boundary conditions by separation of variables.² For arbitrary positive initial conditions,

$$\tilde{f}(t, J) \propto t^{-2}e^{-J/t} \quad \text{as } t \rightarrow \infty. \quad (32)$$

As promised, this has self-similar form: J enters only in the combination J/t [or $J/(D_0 t)$ in dimensionful units]. It can be verified that Eq. (32) is an exact solution of Eq. (31), and its integral over all J is $\propto t^{-1}$, in agreement with our expectation for $P(t)$ at late times.

For other values of the indices α & β satisfying $\alpha < \beta - 1$, we have the following situation. Again, $\bar{\Gamma}$ is negligible at large J , so Eqs. (25) & (27) yield $G(J_1, J_S) \propto 1/D(J_1)$ at $J_1 \gg J_S$. Therefore the integral (28) for the first moment $f_1(J)$ diverges if $\beta \leq 1$, and consequently, the mean lifetime converges only if $\beta > 1$. In other words, the mean lifetime exists only if t_{diff} increases more slowly than $r^{1/2}$.

3.2.1. A useful theorem about the eigenvalue spectrum

The following technical result helps to interpret differences between the late-time behaviors of the planetary distribution in the MMSN and in alpha disks.

The large- t behavior of $f(t, J)$ is dominated by the singularities of $\hat{f}(s, J)$ at largest $\text{Real}(s)$. These correspond to eigenvalues $\{\lambda\}$ obtained by separating variables in Eq. (5) with assumed

²This is eased by the change of variables $x \equiv \sqrt{2J}$ and $g(x) \equiv x\tilde{f}(J)$, which produces the Bessel equation of order one on the righthand side. Hankel transforms can then be used.

time dependence $\exp(-\lambda t)$. If the eigenvalues are real and discrete, $0 < \lambda_1 < \lambda_2 < \dots$, then $f(t, J) \propto f_{\lambda_1}(J) \exp(-\lambda_1 t)$ at late times, where $f_{\lambda}(J)$ is the eigenfunction corresponding to λ . (We assume that these modes are complete.) On the other hand, if the eigenvalue spectrum is continuous and extends to arbitrarily small positive λ , then the late-time decay is slower than exponential, perhaps a power law. Defining

$$g_{\lambda}(J) \equiv \int_J^{\infty} f_{\lambda}(\bar{J}) d\bar{J},$$

and setting $w \equiv e^{\mu}$ and $p \equiv e^{\mu} D$, with μ as in Eq. (15), one can re-cast the separated version of Eq. (5) in self-adjoint Sturm-Liouville form

$$\frac{d}{dJ} \left[p(J) \frac{d}{dJ} g_{\lambda}(J) \right] + \lambda w(J) g_{\lambda}(J) = 0. \quad (33)$$

In all disks of interest to us, $f \rightarrow 0$ as $J \rightarrow 0$ and the integral of f over J is finite, whence $g'_{\lambda}(0) = 0$ and $g_{\lambda}(\infty) = 0$. A theorem of Drábek & Kufner (2005) then asserts that if the limit

$$\lim_{J \rightarrow \infty} \left[\int_0^J w(x) dx \right]^{1/2} \left[\int_J^{\infty} \frac{dx}{p(x)} \right]^{1/2} \quad (34)$$

vanishes, then the spectrum is discrete and positive. [The theorem also requires p and w to be positive and continuous, which is always true for us, and it encompasses “quasilinear” generalizations of Eq. (33).] It is easy to show that in disks where $t_{\text{mig}}/t_{\text{diff}}$ tends to zero as $J \rightarrow 0$ and to infinity as $J \rightarrow \infty$, the limit (34) is equivalent to

$$\lim_{J \rightarrow \infty} \left[J \int_J^{\infty} \frac{d\bar{J}}{D(\bar{J})} \right]^{1/2}. \quad (35)$$

In the MMSN [$D(J) \propto J$], this limit diverges, so a continuous spectrum extending to $\lambda = 0^+$ is allowed and indeed must exist, or else we would not have the self-similar behavior discussed above. In the alpha disks studied numerically in §4, on the other hand, it appears that $t_{\text{diff}} \equiv J^2/D(J) \rightarrow 0$ as $J \rightarrow \infty$ [Fig. (1)], so the limit vanishes and a discrete spectrum is implied. This is clearly true of power-law disks with $\alpha - \beta + 1 < 0$ and $\beta > 2$, so the survival probability $P(t)$ should decay exponentially in these disks. We conjecture that the continuum exists and $P(t)$ follows a power law for all $\beta < 2$, because further consideration of Eqs. (28) indicates that the n^{th} moment of the lifetime exists only if $\beta > 2n/(n+1)$.

4. Numerical method and tests

The diffusion equation (5) with a source term reads:

$$\frac{\partial F_J}{\partial J} = S(t, J) - \frac{\partial f}{\partial t}. \quad (36)$$

We find numerical solutions with an implementation of the generic relaxation code described in Hameury et al. (1998). The finite-difference scheme is fully implicit in time. Given a distribution $f(t, J)$ at time t , we only need to solve the one-dimensional boundary-value problem in J to find the solution at time $t + dt$. We thus relax successively from one solution to another over a variable timestep, dt . Controls over the size of the timestep ensure that, at each grid point, the change in each variable over dt is within an acceptable tolerance. The system is described by two first-order differential equations equivalent to Eq. (36), supplemented with a third differential equation that defines the numerical domain. For simplicity, we do not implement an adaptive mesh but use instead a fixed grid on the numerical domain, chosen to be uniformly spaced in $\log r$. We take as variables the set $(f, \partial(Df)/\partial J, J)$. Numerical stability of the solutions is achieved with centered-differencing schemes for f and J , and an upwind-differencing scheme for $\partial(Df)/\partial J$.

Three boundary conditions are required. The numerical domain extends from the inner edge of the disk, at $\simeq 10^{-2}$ AU, out to 1000 AU. At the inner boundary we trivially set the value of J and are free to fix $f = 0$. At the outer boundary we demand the flux be zero. In steady-state, as discussed in §3.1, this is a boundary condition that must be satisfied if diffusion dominates at large radii. To avoid potential complications near the disk edge, we extend our numerical domain to sufficiently large radii that it does not influence our results.

We have tested our numerical results for power-law models against the analytic steady-state solutions described in §3.1. The numerical solutions converge satisfactorily for a modest grid spacing (typically 1000 grid points over five decades in radius). Additional tests at ten times this resolution show clear numerical convergence of the steady-state results. Agreement with the late-time behavior expected from the time-dependent self-similar solutions described in §3.2 will also be demonstrated below (see Fig. 4).

5. Numerical Solutions

We study the combined effects of migration and diffusion on the orbital evolution of low-mass proto-planets for two separate classes of disk models: the Minimum Mass Solar Nebula (MMSN) and T Tauri alpha disks. The MMSN model adopted here has a mean surface density $\bar{\Sigma} \propto r^{-3/2}$ and an aspect ratio $h/r \propto r^{1/4}$, which are normalized to 4200 g cm^{-2} and 0.1 at $r = 1 \text{ AU}$, respectively. The T Tauri alpha disk model adopted is identical to the irradiated disk described by Menou & Goodman (2004, see their Fig. 1), accreting steadily at a rate $\dot{M} = 10^{-8} M_{\odot} \text{ yr}^{-1}$. We take as our reference model the alpha disk with viscosity parameter $\alpha = 0.02$. For comparison, we also consider a more massive and cooler alpha disk, with $\alpha = 10^{-3}$. The inner edge of the disks is located at 0.01 AU and 0.02 AU in the MMSN and the alpha disks, respectively. The mass of the primary is $1 M_{\odot}$ in the MMSN and $0.5 M_{\odot}$ in the alpha disks. These slight model differences have very little influence on our results. Note that, while the disk models used are assumed to be steady, we are studying the time-dependent orbital evolution of planets embedded in these disks with equation (5). As a consequence, our method can only apply to proto-planets of small enough mass that they

exert a negligible feedback on the disk structure (broadly speaking, $M_p \lesssim 10M_{\oplus}$; e.g. Menou & Goodman 2004).

Turbulence is assumed to be present everywhere in our disk models. The magnitude of the corresponding diffusion coefficient is uncertain through both the amplitude and the correlation time of the turbulent torque fluctuations. We quantify these uncertainties with a single parameter, ϵ . If we define

$$\epsilon \equiv \frac{\tau_c}{\tau_{\text{orb}}} \left(\frac{\mathcal{C}_D}{0.046} \right)^2, \quad (37)$$

then

$$D(J) = \tau_c \times \overline{[\delta\Gamma(t, J)]^2} = \epsilon (2\pi)^3 (0.046)^2 \frac{\bar{\Sigma}^2 J^7}{G^2 M_*^4 M_p^5}. \quad (38)$$

The calibration performed in §2.1 suggests that $\epsilon \simeq 0.5$ is a reasonable value, which we have assumed to be independent of radius. However, we also investigate the effects of varying this parameter by several orders of magnitude.

5.1. General Scalings

It is useful to discuss a few general scalings specific to our disk models before we discuss the details of time-dependent numerical solutions. To quantify the relative importance of diffusion *vs.* migration in the models, we define a local diffusion time $t_{\text{diff}} = J^2/D \propto \bar{\Sigma}^{-2} J^{-5} \propto J^{-4k-5}$ (for $\bar{\Sigma} \propto r^k$) and a local migration time, $t_{\text{mig}} = J/|\bar{\Gamma}| \propto h^2 \bar{\Sigma}^{-1} J^{-5} M_p^{-1}$, according to Eq. (10), so that $t_{\text{mig}} \propto J^3 M_p^{-1}$ in the MMSN. The ratio of these timescales has a particularly simple dependence upon disk and planetary properties:

$$\frac{t_{\text{mig}}}{t_{\text{diff}}} \propto \frac{h^2 \bar{\Sigma}}{M_p}. \quad (39)$$

One expects the evolution of planets located in regions of a disk with $t_{\text{mig}} \ll t_{\text{diff}}$ to be dominated by migration and vice-versa. While the diffusion time is independent of planet mass, the migration time is inversely proportional to M_p . Therefore, lower mass proto-planets will be more sensitive to the effects of turbulent torque fluctuations. In addition, the two timescales differ in their dependence on the mean surface density, $\bar{\Sigma}$, which tends to make planets in denser disks more susceptible to the effects of diffusion. As we shall now see, a general consequence of these scalings is that one expects the effects of diffusion to dominate only in the outer regions of proto-planetary disks (at least for the classes of disk models considered here).

Figure 1 shows profiles of various important quantities in the MMSN and our two alpha disk models. Panel I shows profiles of mean surface density, $\bar{\Sigma}$. Both the slope and normalization of $\bar{\Sigma}$ profiles matter for the relative importance of migration *vs.* diffusion. Panels III and IV show profiles of local migration and diffusion times in the various disk models. While t_{diff} increases linearly with J ($\propto r^{1/2}$) in the MMSN, it decreases with increasing radius in the alpha disk models.

This is a consequence of the steeper $\bar{\Sigma}$ profile in the MMSN. The profiles of t_{mig} , derived from Eq. (10) for the MMSN and from the detailed calculations³ of Menou & Goodman (2004) for the alpha disk models, show local migration times which decrease toward small radii in both classes of models. Finally, panel II shows the ratio of timescales, $t_{\text{mig}}/t_{\text{diff}}$, which is important to characterize the behavior of planets embedded in these disks. As mentioned earlier, in all three models, this ratio grows above unity (indicated by the horizontal dash-dotted line in panel II) only at radii $\gtrsim 10$ AU if $M_p \lesssim 1 M_{\oplus}$, indicating that diffusion should dominate over migration only in the outer regions of these disks (and this despite the increasing value of t_{diff} with radius in the MMSN).

Although very useful, the profiles shown in Figure 1 do not capture all of the complexity of the migration-diffusion problem. First, all the quantities plotted in panels II-III-IV were derived for a planet mass $M_p = 1 M_{\oplus}$ and a torque fluctuation normalization $\epsilon = 0.5$. The profiles are easily rescaled for different values of these parameters (as indicated by labels in Fig. 1), but it is clear that the exact location of the transition from migration- to diffusion-dominated evolution depends on the proto-planetary disk model adopted, the value of the planet mass, and the normalization ϵ of the diffusion coefficient. Nevertheless, the dominance of diffusion over migration in the outer regions of these disks is robust because $\bar{\Sigma}h^2$ tends to increase with radius in disk models of interest [Eq. (39)].

Secondly, as shown in panel III, in a disk model with realistic opacities, sudden and non-monotonic variations in the value of t_{mig} at radii $\lesssim 3$ AU could complicate the orbital evolution of planets substantially, by stalling their migration as they reach the disk inner regions. This is best explored with global numerical solutions of the time-dependent Fokker-Planck equation, as seen in §5.2.

A third complication arises from the radial dependence of the diffusion driven by turbulent torque fluctuations. As mentioned in §2, the radial variation of the diffusion coefficient leads to an additional contribution to the advected flux of planets. Since $-\partial D/\partial J \propto -(7 + 4k) J^{6+4k}$ for $\bar{\Sigma} \propto r^k$, and since $k = -3/2$ in the MMSN and $k > -3/2$ in the alpha disk models, this additional term tends to advect planets inward in all the disk models considered. We can define a local advection timescale associated with this new contribution, $J/(\partial D/\partial J)$, and compare it to the values of t_{mig} and t_{diff} defined above. We find that this advection timescale is everywhere exactly equal to t_{diff} in the MMSN, while it is shorter than t_{diff} everywhere in our alpha disk models (as shown explicitly for the $\alpha = 0.02$ case by the short-dashed line in panel IV of Fig. 1). Consequently, even in disk regions where diffusion nominally dominates over migration in our models (as measured by the ratio $t_{\text{diff}}/t_{\text{mig}}$), this additional contribution due to radially inhomogeneous diffusion should still cause a rather significant effective advection of planets towards the star.

³Specifically, we use the 3D model in which the gas is assumed to be vertically extended over a full disk scale height for the torque calculation.

5.2. Continuous and Burst Formation of Planets

We have studied two different types of time-dependent models for the diffusive migration of planets in proto-planetary disks, corresponding approximately to a continuous and a burst scenario for planet formation. In both cases, for the sake of clarity, the source of planets was localized, taking the form of a sharply peaked Gaussian approximating the delta source function of Eq. (13). We have verified that our results do not depend sensitively on the detailed shape of the Gaussian source function adopted. As we shall see, the predictions for these rather different scenarios for planet formation are broadly consistent with each other.

Figure 2 shows steady-state distributions obtained by numerically solving Eq. (36) with a source term centered at $r_S = 10$ AU, steadily producing earth-mass planets at a rate $\Lambda = (10^5 \text{ yr})^{-1}$. The topmost curve in each panel is the steady-state distribution. The enclosed curves, on the other hand, are snapshots of the decaying distributions at selected time intervals after the source is shut off. We have verified that the steady-state distributions for the MMSN in Panels I and III are fully consistent with the analytic solution, Eqs. (15)-(16), for power-law disks. A fiducial normalization of $\epsilon = 0.5$ for torque fluctuations is assumed in all cases except in panel III, where $\epsilon = 0.02$ has been scaled down to extend the migration-dominated regime out to ~ 10 AU in the MMSN. Thus, at 10 AU, the disks in Panels I and IV are diffusion-dominated and the disks in Panels II and III are migration-dominated.

The distinction between diffusion-dominated and migration-dominated evolutions is most clearly illustrated by comparing panels I and III. While the initial steady-state peaked distribution is eroded and advected for the most part in panel III, with little diffusion at large radii, there is significantly more diffusion at large radii in panel I. That distinction is not as clear in the alpha disk models, however. Note that, in both panels II and IV, the initial steady-state distribution is strongly peaked not at the source radius, but at radii where migration stalls (as seen from panel III in Fig. 1). In addition, even though diffusion is more important in the model with $\alpha = 10^{-3}$ in panel IV, the effect appears to be minor in smoothing out only slightly the same sharp distribution features as in panel II. This is partly explained by the strong contribution of radially inhomogeneous diffusion to inward advection of planets, which is always important in our alpha disk models (as explained in the previous subsection). Even though diffusion is equally important at $r_S = 10$ AU in the models of panel I and IV (see $t_{\text{mig}}/t_{\text{diff}}$ in Fig. 1), it is more inhomogeneous in the alpha disk model and thus promotes a significantly more efficient inward advection of planets.

Our models with a burst of planet formation confirm these general trends. To study this formation scenario, we solve the diffusion equation (5) without source term and impose a specific initial condition for the distribution of planets at $t = 0$ instead. The initial distribution, $f(t = 0, J) = f_i(J)$, is modeled as a narrow Gaussian centered on $J_S = M_p \sqrt{GM_* r_S}$. Figure 3 shows the evolution of such distributions of Earth-mass planets initially located at $r_S = 10$ AU in the same four disk models as in Fig. 2.

As before, a comparison between the two MMSN models shows that the effects of diffusion are

much more important in the model with $\epsilon = 0.5$ (panel I) than in the one with $\epsilon = 0.02$ (panel III). In particular, a sub-population of planets diffusing at large radii is clearly visible in panel I. On the contrary, while diffusion still acts to widen the initial distribution in panel III, the dominant effect is a global advection of the distribution of planets. Finally, in agreement with our previous results, Figure 3 shows that the most significant feature of alpha disk models is the effect of rapid variations in the migration rates of planets, which causes them to stall at specific locations in the disk and results in time-varying peaks in the distributions of panels II and IV. Even though diffusion is comparatively as important in panels I and IV, at 10 AU, its effects appear to be much less important in the alpha disk model of panel IV. We attribute this difference, once again, to the more inhomogeneous diffusion in alpha disk models, which contributes substantially to the inward advection of planets into regions of the disk where diffusion becomes gradually less important and the effects of stalling radii are felt more strongly.

5.3. Radial Excursions and Lifetimes

Two important aspects of the orbital evolution of planets which are not well captured by Figure 3 are the properties of the surviving minority of planets at late times and large radii, and the representative planetary lifetimes in burst-formation models.

The fraction of planets that diffuse to orbital radii greater than their formation radius, r_S , can be characterized by the time-dependent quantity

$$\chi_a(t) = \int_{J_a}^{\infty} f(t, J) dJ \left/ \int_0^{\infty} f(0, J) dJ \right., \quad (40)$$

where J_a is the angular momentum at a fiducial radius a [AU] $> r_S$. Hereafter, the integral over the initial distribution appearing in the denominator of Eq. (40) will be normalized to unity. The maximum values of $\chi_{20}(t)$ and $\chi_{100}(t)$, reached typically just after the majority of planets were accreted by the star, are listed in Table 1 for the four models of Figure 3. Not surprisingly, models with a strong role for diffusion tend to have a fairly large maximum fraction of planets diffusing beyond 20 AU ($\sim 10\%$) and 100 AU ($\sim 1\%$), while models with little diffusion have much reduced maximum fractions of planets at large radii ($\lesssim 0.01\%$ beyond 20 AU, $\lesssim 10^{-6}$ beyond 100 AU).

Table 1: Maximum fraction of planets beyond $a = 20$ AU and 100 AU in the four models of Figure 3

Disk Model	Torque Fluctuations	χ_{20}^{\max}	χ_{100}^{\max}
MMSN	$\epsilon = 0.5$	1.4×10^{-1}	3.4×10^{-2}
Alpha-Disk ($\alpha = 0.02$)	$\epsilon = 0.5$	1.9×10^{-4}	1.4×10^{-6}
MMSN	$\epsilon = 0.02$	1.0×10^{-4}	7.6×10^{-8}
Alpha-Disk ($\alpha = 10^{-3}$)	$\epsilon = 0.5$	7.4×10^{-2}	9.7×10^{-3}

We compute three additional time-dependent quantities to help us better characterize the

properties of surviving planets in our models. The first is the survival probability, computed as

$$P(t) = \int_0^\infty f(t, J) dJ.$$

The second is the median orbital radius of surviving planets, $r_{\text{med}}(t)$, defined by

$$\int_0^{M_p \sqrt{GM_* r_{\text{med}}(t)}} f(t, J) dJ = \frac{1}{2} P(t).$$

Finally, since the mean lifetime is often ill-defined (§3.2), we calculate the median lifetime t_m defined by $P(t_m) = 1/2$.

Figure 4 shows how the survival probability and the median radius of surviving planets evolve with time in burst formation models for Earth-mass planets in the MMSN. Three separate models with burst formation at $r_S = 1, 10$ and 100 AU are shown for comparison (solid lines). Note that the middle solid line corresponds to the exact same model as the one shown in panel I of Figure 3. For reference, vertical dotted lines bracket typical lifetimes for gaseous proto-planetary disks (10^6 – 10^7 yrs; e.g. Haisch et al. 2001). The median lifetime of the population of planets, which is such that $P(t) = 0.5$, is indicated by a horizontal dash-dotted line in the upper panel. The lifetimes differ substantially in the three models shown, from much shorter to somewhat longer than the typical disk lifetimes. The self-similar $P(t) \propto t^{-1}$ behavior predicted in §3.2 is indeed achieved at late times in the three models. As shown in the lower panel of Figure 4, the median radius of surviving planets does not evolve much at early times and remains close to the formation radius, as the distribution of planets mostly diffuses out to both small and large radii. Once a significant fraction of planets have been accreted by the central star, however, the surviving planets are found at a median radius increasing almost quadratically with time independently of where they were formed. This is just what one would expect from the self-similar solution (32): $r_{\text{med}}^{1/2} \propto J_{\text{med}} \rightarrow D_0 t \ln 2$.

Figure 5 shows the evolution of the same two quantities in burst formation models for Earth-mass planets in the alpha disk (with $\alpha = 0.02$) this time. Six separate models with burst formation at $r_S = 1, 5, 10, 20, 100$ and 500 AU are shown for comparison (solid lines). Note that the fourth solid line from the top corresponds to the exact same model as the one shown in panel II of Figure 3. The results are qualitatively consistent with the MMSN ones, with a few important differences. There is no self-similar behavior at late times in this case and the more dominant role of advection in the alpha disk model tends to make the median radius of surviving planets move inward initially, until the majority of them are lost to the central star. Among the surviving minority, however, r_{med} asymptotes to ~ 50 AU at late times, independently of the formation radius, r_S . This behavior is explicable if, as predicted by the theorem cited in §3.2.1, the eigenmodes of Eq. (5) are discrete: then $f(t, J)$ converges upon the most slowly decaying mode, and $r_{\text{med}}(t)$ tends to the median radius of this eigenmode. Figures 1 and 5 suggest that this radius is close to that at which $t_{\text{mig}}^{-1} + t_{\text{diff}}^{-1}$ [more accurately, $t_{\text{mig}}^{-1} + t_{\text{adv}}^{-1}$, where $t_{\text{adv}} \equiv J/(\partial D/\partial J)$] is minimized, as might be expected since

planets should linger longest where the combined effects of diffusion and migration are weakest. In the MMSN, both timescales increase without limit as $J \rightarrow \infty$, and the spectrum of eigenmodes is apparently continuous.

It is also worth emphasizing that the largest peak value of t_{mig} at sub-AU distances in alpha disk models (see panel III in Fig. 1) effectively limits the migration time of Earth-mass planets into their star to values $\gtrsim 10^7$ yrs (for $\alpha = 0.02$), which exceeds typical disk lifetimes.

Based on this general understanding of diffusive migration in our burst-formation models, let us now focus more systematically on several important model dependencies. Figure 6 illustrates how the median lifetimes of Earth-mass planets formed at different radii in the MMSN and the alpha disk are affected by changes in the normalization of torque fluctuations, ϵ . For the nominal $\epsilon = 0.5$ value adopted (indicated by a vertical dash-dotted line in Fig. 6), diffusion mostly affects the orbital evolution of planets formed at the largest radii, by reducing somewhat their median lifetime. As ϵ is increased above this nominal value, the trend becomes clearer. Median lifetimes for all formation radii are considerably reduced at larger values of ϵ , more so in the MMSN than in the alpha disk. The long-dashed line in Figure 6 results when we neglect the mean torque $\bar{\Gamma}$ in the governing equation (5). The convergence of the solid curves for the alpha-disk model to a value independent of r_S is related to the value of the diffusion time, t_{diff} , at the disk inner boundary. For sufficiently large ϵ , $t_{\text{diff}} \ll t_{\text{mig}}$ everywhere on the grid. But t_{diff} increases toward small radius in the alpha disks (Fig. 1). So the median lifetime in the large- ϵ regime is comparable to t_{diff} at the inner boundary, r_{min} ; we have verified that t_{med} decreases as r_{min} is increased. Nevertheless, in all cases, the effect of diffusion is to reduce the median lifetime.

Figure 7 illustrates how the median lifetimes of planets of various masses, all formed at $r_S = 10$ AU in the MMSN and in the alpha disk, are affected by changes in the normalization of torque fluctuations, ϵ . For the nominal $\epsilon = 0.5$ value, diffusion mostly affects the orbital evolution of the lower mass planets, and reduces somewhat their median lifetimes. This results from the larger values of t_{mig} at lower planet mass, whereas t_{diff} is independent of planet mass. As ϵ is increased, diffusion progressively dominates and the distinction among planets of various masses gradually disappears. For large enough values of ϵ , the median lifetime of all planets with masses $M_p \lesssim 10M_{\oplus}$ formed at $r_S = 10$ AU is reduced below typical disk lifetimes. As in the previous figure, however, the lifetimes for $\epsilon \gg 1$ in the alpha disk are dominated by the diffusion time at the inner boundary.

6. Discussion and Conclusion

As anticipated by Nelson & Papaloizou (2004), Laughlin et al. (2004), and Nelson (2005), our Fokker-Planck treatment confirms that diffusion driven by turbulent torque fluctuations in proto-planetary disks can greatly influence the orbital evolution of embedded low-mass protoplanets. Contrary to some expectations, diffusion does not promote planetary survival but instead systematically reduces the lifetime of most planets in the disk. However, it does help a small

fraction of planets diffuse to large radii where they can survive for extended periods. (We consider that a planet “survives” if its orbit remains larger than the inner edge of the disk.)

Our results point to a potentially important role for non-deterministic effects in planet formation scenarios. In models with a significant level of diffusion, most proto-planets in the Earth-mass range could end up being accreted by their stars, while only a small fraction of them would survive by diffusing to large radii. In scenarios where all proto-planetary disks are efficient at forming planets, this could be interpreted as leading to only a fraction of all potential host stars being successful in keeping a system of surviving planets. Even systems starting with very similar initial conditions may end up with very different planetary orbital configurations once their gaseous disks disappear.

Neglecting the effects of direct gravitational interactions between proto-planets, which are likely to happen from differential rates of migration and diffusion, is one of many model limitations in our work. We have already mentioned that our study is restricted to proto-planets of low enough masses that they do not affect in any way the structure of their host disk. This excludes the late stages of giant planet formation, which are obviously of considerable interest. In particular, it has been suggested that migration and diffusion, each independently, could accelerate the rate of growth of cores until they reach the critical mass at which runaway envelope accretion occurs (e.g. Rice & Armitage 2003; Alibert et al. 2005a,b). Studying these possibilities within the context of global models such as ours would be interesting.

Even within the strict regime of applicability of our models, significant uncertainties exist. Let us mention a few. We have focused our work on strictly circular orbits. We have assumed that the underlying proto-planetary disk structure does not evolve with time, and that the amplitude $\delta\Sigma/\Sigma$ of surface-density fluctuations is constant with radius. We have assumed that torque fluctuations can simply be added to a laminar mean torque which is not modified by the turbulence. The laminar torque itself is calculated from a simple extension of the two-dimensional Lindblad torque theory, which does not account for the role of corotation torques.

Despite all these uncertainties, we believe that our results should be broadly valid, provided that turbulence and torque fluctuations in proto-planetary disks satisfy the various stochasticity criteria enunciated in §2. Understanding better the nature of turbulence in proto-planetary disks and in particular indications for long-term correlations in MHD simulations may turn out to be crucial in this context. We would like to issue a plea to the simulation community to study these questions, and in particular, whether the dimensionless amplitude and correlation time of density and torque fluctuations depend only upon the strength of the turbulence (*via* α) or upon the thickness h/r as well (§2.1). The answers will matter both quantitatively (in determining the relative importance of migration *vs.* diffusion in global models such as ours) and qualitatively (in justifying a Fokker-Planck approach or in falsifying it).

We have seen that details of the protoplanetary disk structure (MMSN *vs.* alpha disks) do influence our results at the quantitative level. In that respect, the possibility that a magnetically

layered structure with quiescent dead zones exists in weakly-ionized regions of proto-planetary disks (Gammie 1996; Glassgold et al. 1997; Balbus & Hawley 1998; Fromang et al. 2002; Ilgner & Nelson 2006) may be important. Indeed, the results of Fleming & Stone (2003) suggest that the nature of turbulence in dead zones differs qualitatively from that in MHD turbulent regions, perhaps leading to comparatively reduced torque fluctuations (see also Matsumura & Pudritz 2003, for other suggested effects of dead zones in planet formation scenarios).

The general tendency for a fraction of planets to diffuse to large radii in proto-planetary disks may have consequences of some observational relevance. We note, for instance, that Veras & Armitage (2004) have looked into scenarios for outward planet migration in an attempt to explain observed structures in dust disks as resulting from perturbations by planets located at radii beyond those at which they are thought to be able to form. Rather than invoking outward migration, this may be expected in scenarios with a prominent role for diffusion, as illustrated by our various models.

Acknowledgments

We thank Richard Nelson for help with understanding his simulations. This material is based on work supported in part by the National Aeronautics and Space Administration under Grant NAG5-11664 issued through the Office of Space Science.

REFERENCES

Alibert, Y., Mordasini, C., Benz, W. & Winisdoerffer, C. 2005a, *A&A*, 434, 343

Alibert, Y., Mousis, O., Mordasini, C. & Benz, W. 2005b, *ApJ*, 626, L57

Armitage, P. J. & Rice, W. K. M. (2006), to appear in *A Decade of Extrasolar Planets Around Normal Stars* ([astro-ph/0507492](#))

Balbus, S. A. & Hawley, J. F. 1998, *Rev. Mod. Phys.*, 70, 1

Beaulieu, J.-P. et al. 2006, *Nature*, 439, 437

Bender, C. M. & Orszag, S. A. 1978, *Advanced Mathematical Methods for Scientists and Engineers* (New York: McGraw-Hill)

Brandenburg, A., Nordlund, A., Stein, R. F., & Torkelsson, U. 1995, *ApJ*, 446, 741

D'Angelo, G., Kley, W. & Henning, T. 2003, *ApJ*, 586, 540

Drábek, P. & Kufner, A., 2005, *Proc. Am. Math. Soc.*, 134 (1), 235.

Fleming, T. & Stone, J. M. 2003, *ApJ*, 585, 908

Fromang, S. & Nelson, R. P. 2005, *MNRAS*, 364, L81

Fromang, S., Terquem, C. & Balbus, S. A. 2002, *MNRAS*, 329, 18

Gammie, C. F. 1996, *ApJ*, 457, 355

Gilliland, R. L. et al. 2000, *ApJ*, 545, L47

Glassgold, A. E., Najita, J. & Igea, J. 1997, *ApJ*, 480, 344 [Erratum: 485, 920]

Goldreich, P. & Tremaine, S. 1980, *ApJ*, 241, 425

Goldreich, P. & Sari, R. 2003, *ApJ*, 585, 1024

Haisch, K. E., Lada, E. A. & Lada, C. J. 2001, *ApJ*, 553, L153

Hameury, J.-M., Menou, K., Dubus, G., Lasota, J.-P., & Huré, J.-M. 1998, *MNRAS*, 298, 1048

Hawley, J. F., Gammie, C. F., & Balbus, S. A. 1995, *ApJ*, 440, 742

Hayashi, C. 1981, *Prog. Theor. Phys. Suppl.*, 70, 35

Ilgner, M. & Nelson, R. P. 2006, *A&A*, 445, 205

Johansen, A. & Klahr, H. 2005, *ApJ*, 634, 1353

Kley, W., D'Angelo, G. & Henning, T. 2001, *ApJ*, 547, 457

Korycansky, D. G. & Pollack, J. B. 1993, *Icarus*, 102, 150

Laughlin, G., Steinacker, A., & Adams, F. C. 2004, *ApJ*, 608, 489

Lin, D. N. C., Bodenheimer, P. & Richardson, D. C. 1996, *Nature*, 380, 606

Lin, D. N. C. & Papaloizou, J. 1986, *ApJ*, 309, 846

Lufkin, G. et al. 2004, *MNRAS*, 347, 421

Marcy, G. W., Cochran, W. D. & Mayor, M. 2000, in *Protostars and Planets IV* (Tucson: University of Arizona Press), eds. Mannings, V., Boss, A.P., Russell, S. S.), p. 1285

Matsumura, S. & Pudritz, R. E. 2003, *ApJ*, 598, 645

Menou, K. & Goodman, J. 2004, *ApJ*, 606, 520

Mizuno, H. 1980, *Prog. of Theor. Phys.* 64, 544

Nelson, R. P. 2005, *A&A*, 443, 1067 (N2005)

Nelson, A. F. & Benz, W. 2003a, *ApJ*, 589, 556

Nelson, A. F. & Benz, W. 2003b, *ApJ*, 589, 578

Nelson, R. P. & Papaloizou, J. C. B. 2004, *MNRAS*, 350, 849

Papaloizou, J. C. B. & Terquem, C. 1999, *ApJ*, 521, 823

Papaloizou, J. C. B. & Terquem, C. 2006, *Rep. Prog. Phys.* 69, 119

Pollack, J. B. et al. 1996, *Icarus*, 124, 62

Rice, W. K. M. & Armitage, P. J. 2003, *ApJ*, 598, L55

Safronov, V. S. 1969, *Evoliutsiia doplanetnogo oblaka i obrazovanie Zemli i planet* (Moscow: Nauka) (English transl. *Evolution of the Protoplanetary Cloud and Formation of the Earth and Planets* [NASA Tech. Transl. F-677] [Jerusalem: Israel Program Sci. Transl.] [1972])

Sano, T., Inutsuka, S., Turner, N., & Stone, J.M. 2003, *ApJ*, 605, 321.

Santos N. C., Israelian G., Mayor M. 2004, *A&A*, 415, 1153

Sato, B. et al. 2005, *ApJ*, 633, 465

Schaefer, C., Speith, R., Hipp, M., Kley, W. 2004, *A&A*, 418, 325

van Kampen, N. G. 1981, *Stochastic Processes in Physics and Chemistry* (Amsterdam: North-Holland)

Veras, D. & Armitage, P. 2004, *MNRAS*, 347, 613

Ward, W. R. 1997a, *Icarus*, 126, 261

Ward, W. R. 1997b, *ApJ*, 482, L211

Weldrake, D .T. F., Sackett, P. D., Bridges, T. J.& Freeman, K. C. 2005, *ApJ*, 620, 1043

Wuchterl, G., Guillot, T. & Lissauer, J. J. 2000, in *Protostars and Planets IV* (Tucson: University of Arizona Press) eds. Mannings, V., Boss, A.P., Russell, S. S., p. 1081

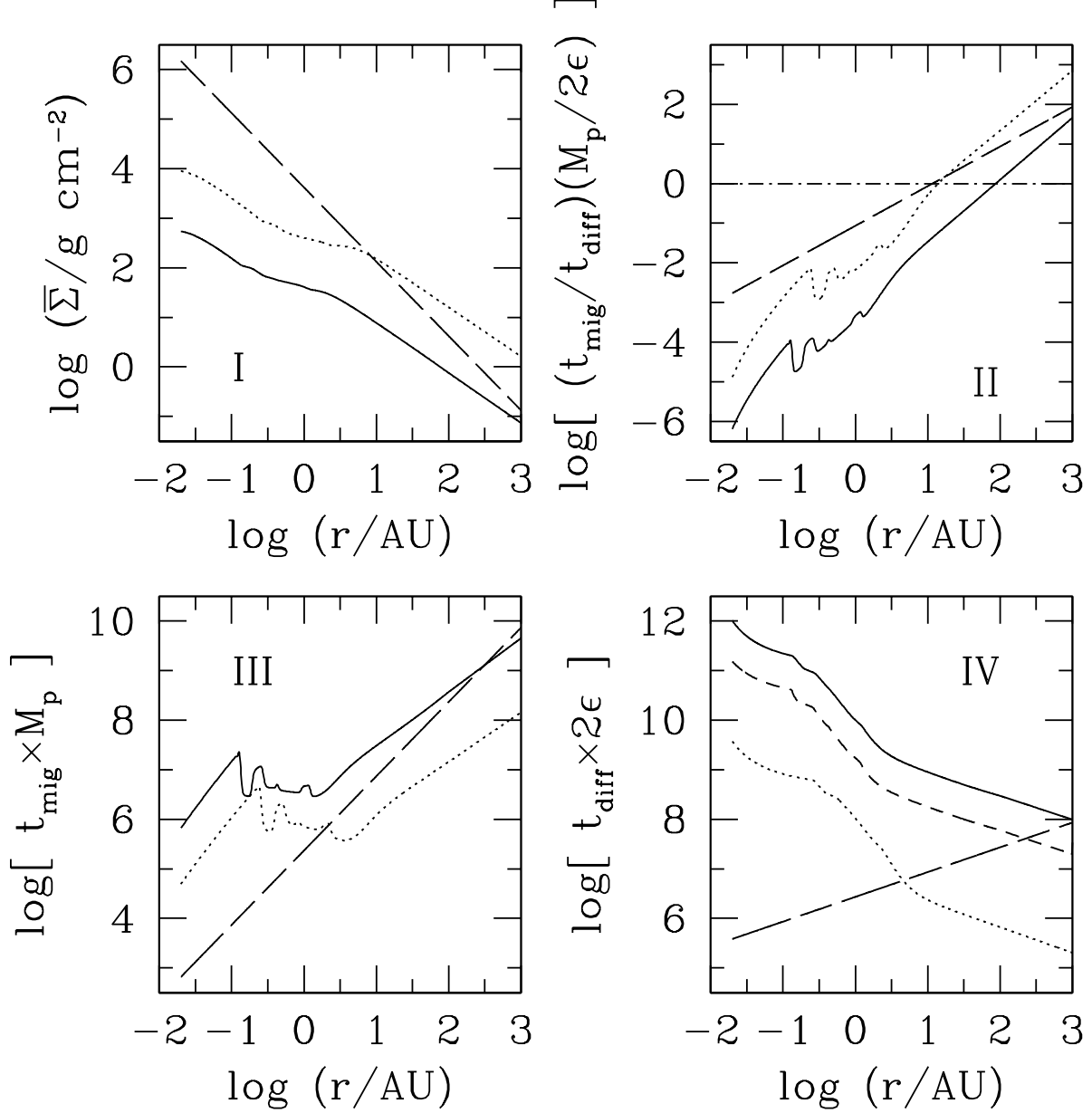


Fig. 1.— In all four panels, quantities were plotted assuming a planet mass $M_p = 1M_\oplus$ and torque fluctuations normalized to $\epsilon = 0.5$. The long-dashed lines correspond to the MMSN, while the solid and dotted lines correspond to the $\alpha = 0.02$ and $\alpha = 10^{-3}$ T Tauri alpha-disk models, respectively. Panel I shows mean surface density profiles. Panel II shows ratio of local migration time to local diffusion time in the three models. The horizontal dash-dotted line indicates the formal transition between migration-dominated and diffusion-dominated regime for Earth-mass planets. Panels III and IV show local migration times and local diffusion times, respectively. The short-dashed line in Panel IV corresponds to the local advection timescale due to inhomogeneous diffusion, $J/(\partial D/\partial J)$, for the $\alpha = 0.02$ alpha-disk model.

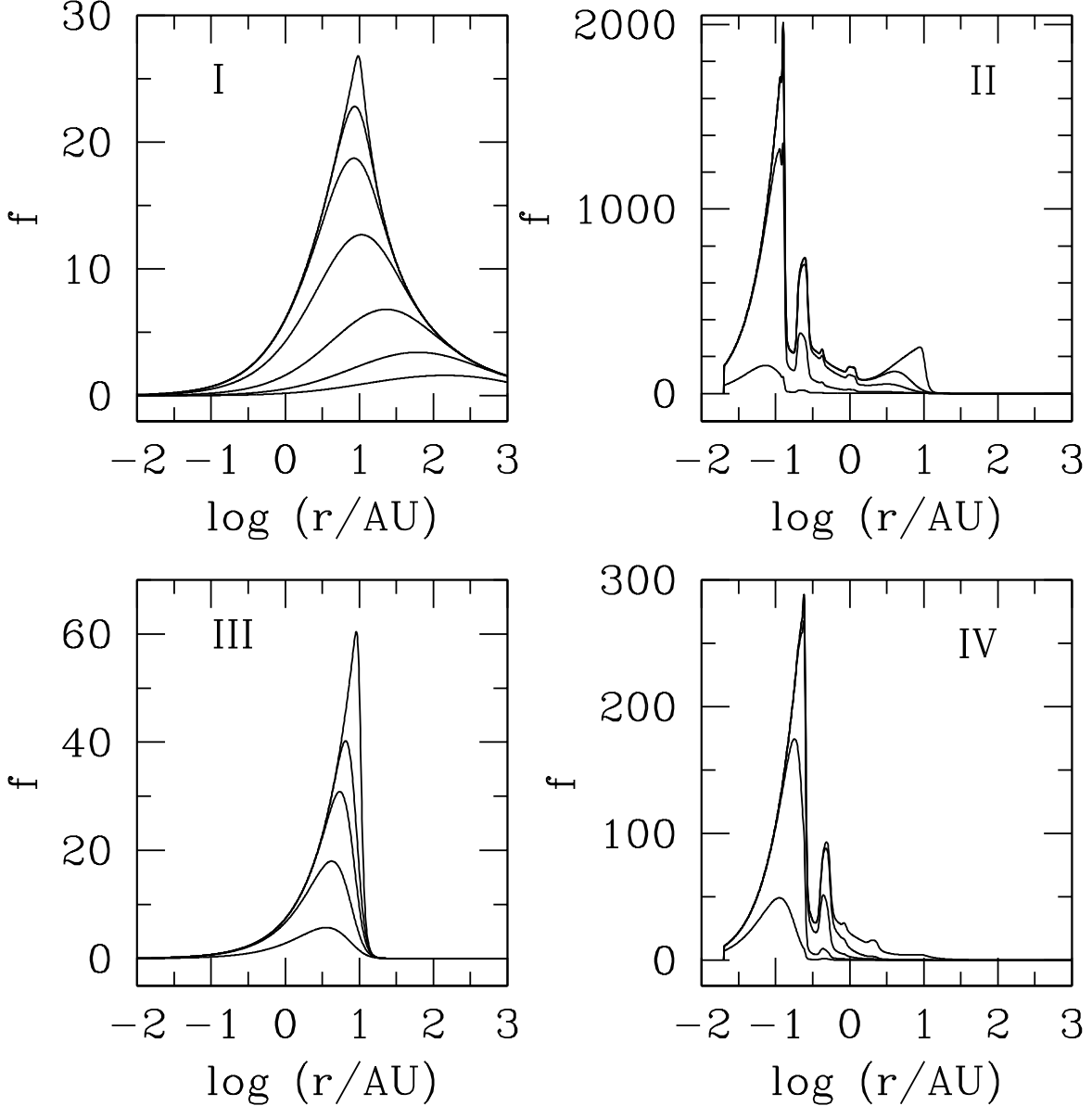


Fig. 2.— Snapshots of the decay of steady-state distributions after source shut-off. In each case, the source formed Earth-mass planets at $r_S = 10$ AU at a rate $\Lambda = (10^5 \text{ yr})^{-1}$ until shut-off. The disk model in Panels I and III is the MMSN with torque fluctuations normalized to $\epsilon = 0.5$ and 0.02, respectively. The disk models in Panels II and IV are alpha disks with viscosity parameters $\alpha = 0.02$ and 10^{-3} , respectively ($\epsilon = 0.5$). Snapshots are shown at the following times after source shut-off, in log-years: (I) 5,5.5,6,6.5,7,7.5; (II) 6.8,7,7.2,7.4; (III) 5.8,6,6.2,6.4; (IV) 5.8,6,6.2,6.4.

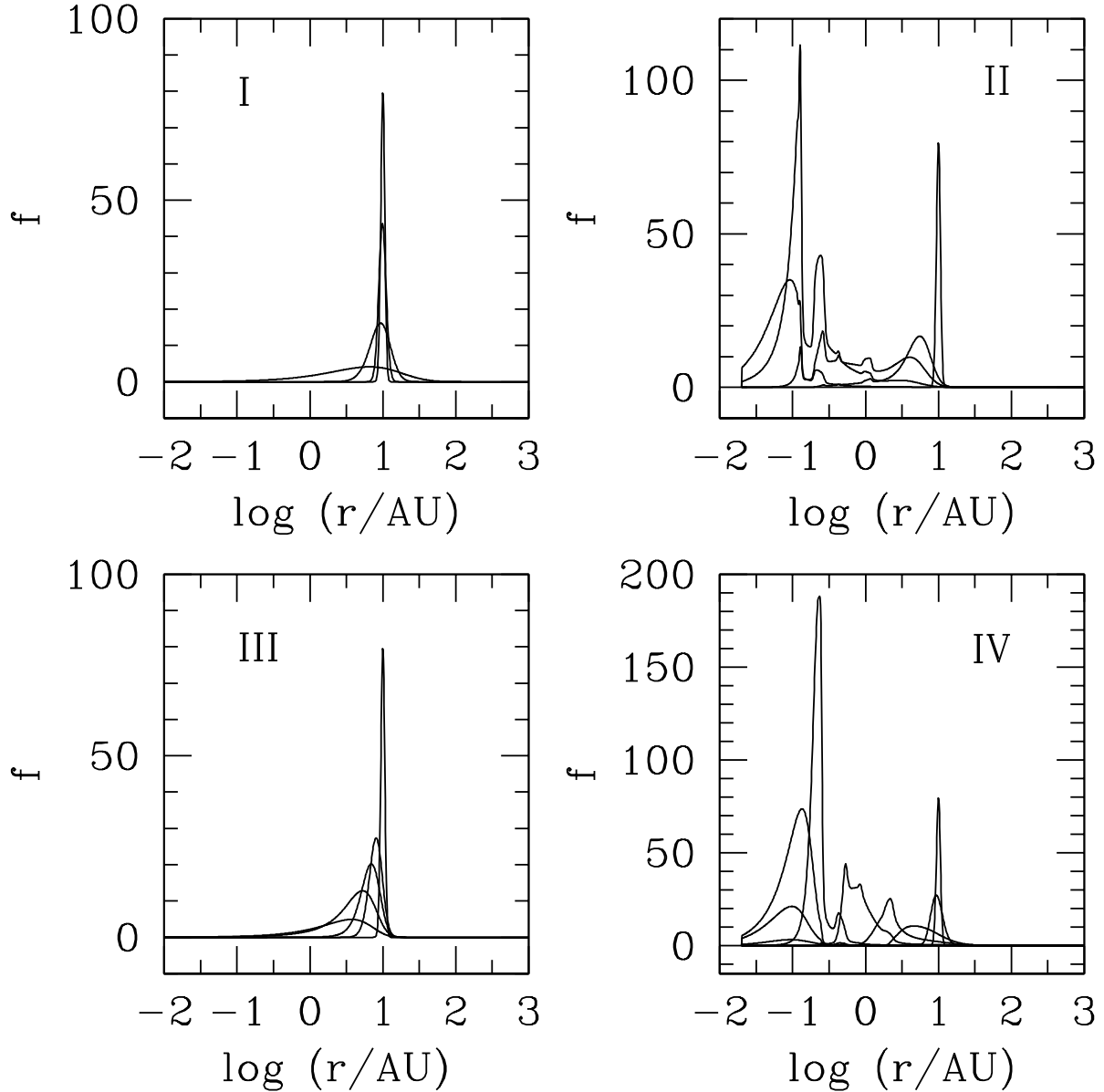


Fig. 3.— Snapshots of the evolution of initially spiked distributions corresponding to a burst of Earth-mass planet formation at $r_S = 10$ AU. The disk model in Panels I and III is the MMSN with torque fluctuations normalized to $\epsilon = 0.5$ and 0.02 , respectively. The disk models in Panels II and IV are alpha disks with viscosity parameters $\alpha = 0.02$ and 10^{-3} , respectively ($\epsilon = 0.5$). Snapshots are shown at the following times after burst formation, in log-years: (I) 4,5,6; (II) 6.8,7,7.2,7.4; (III) 5.8,6,6.2,6.4; (IV) 4,5,5.4,5.8,6.2,6.4,6.5,6.6.

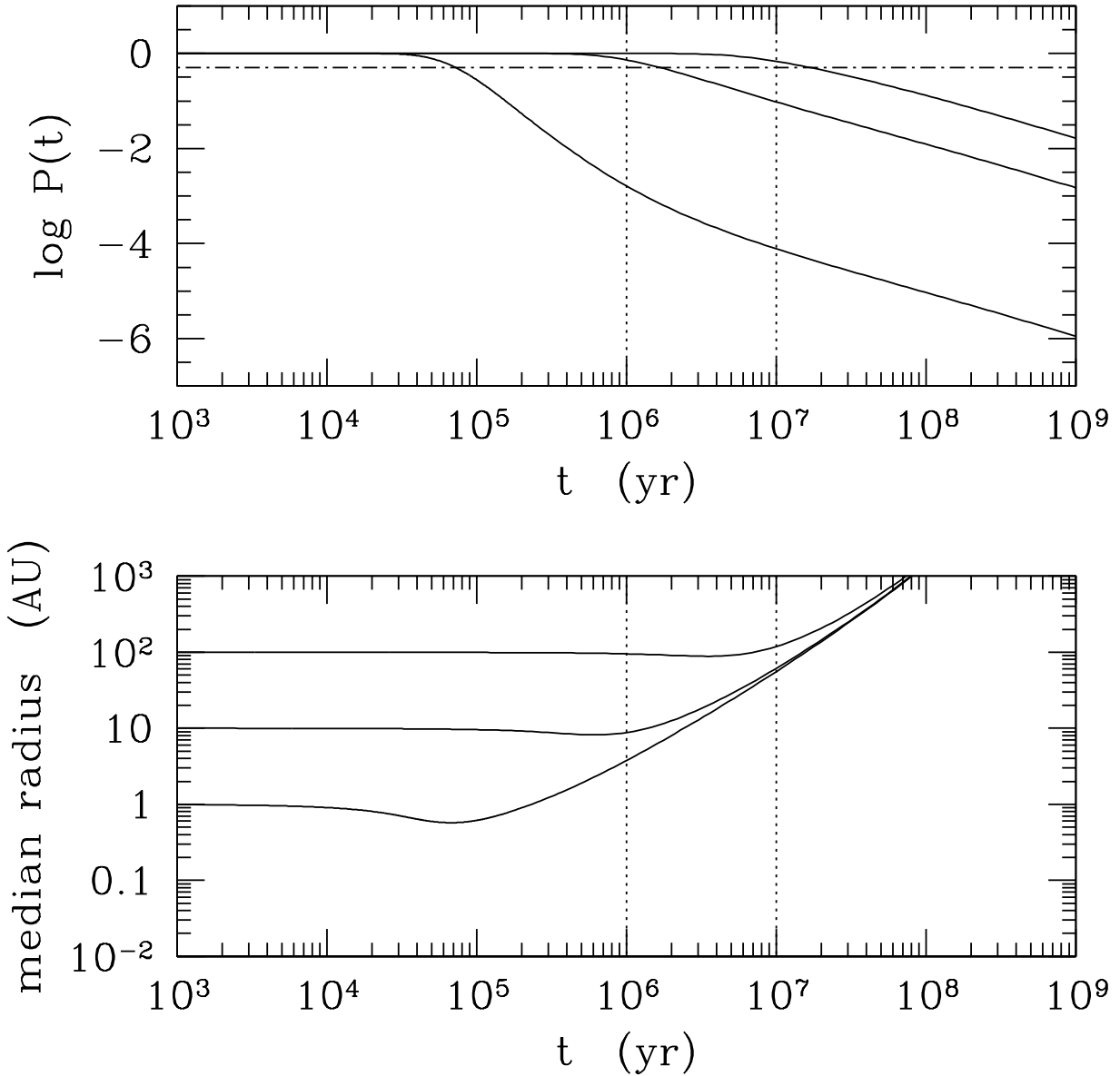


Fig. 4.— Evolution of the survival probability, P (upper panel), and of the median radius of surviving planets (lower panel) for Earth-mass planets formed in a localized burst at $t = 0$ in the MMSN. Torque fluctuations were normalized to $\epsilon = 0.5$. In each panel, the three solid lines correspond to planets formed at $r_S = 100, 10$ and 1 AU (from top to bottom). Vertical dotted lines bracket typical protoplanetary disk lifetimes. The horizontal dash-dotted line in the upper panel corresponds to $P(t) = 0.5$, which defines the median lifetime of planets. A declining fraction of planets survives for long times at increasingly large radii, in agreement with the self-similar $P(t) \propto t^{-1}$ scaling predicted analytically.

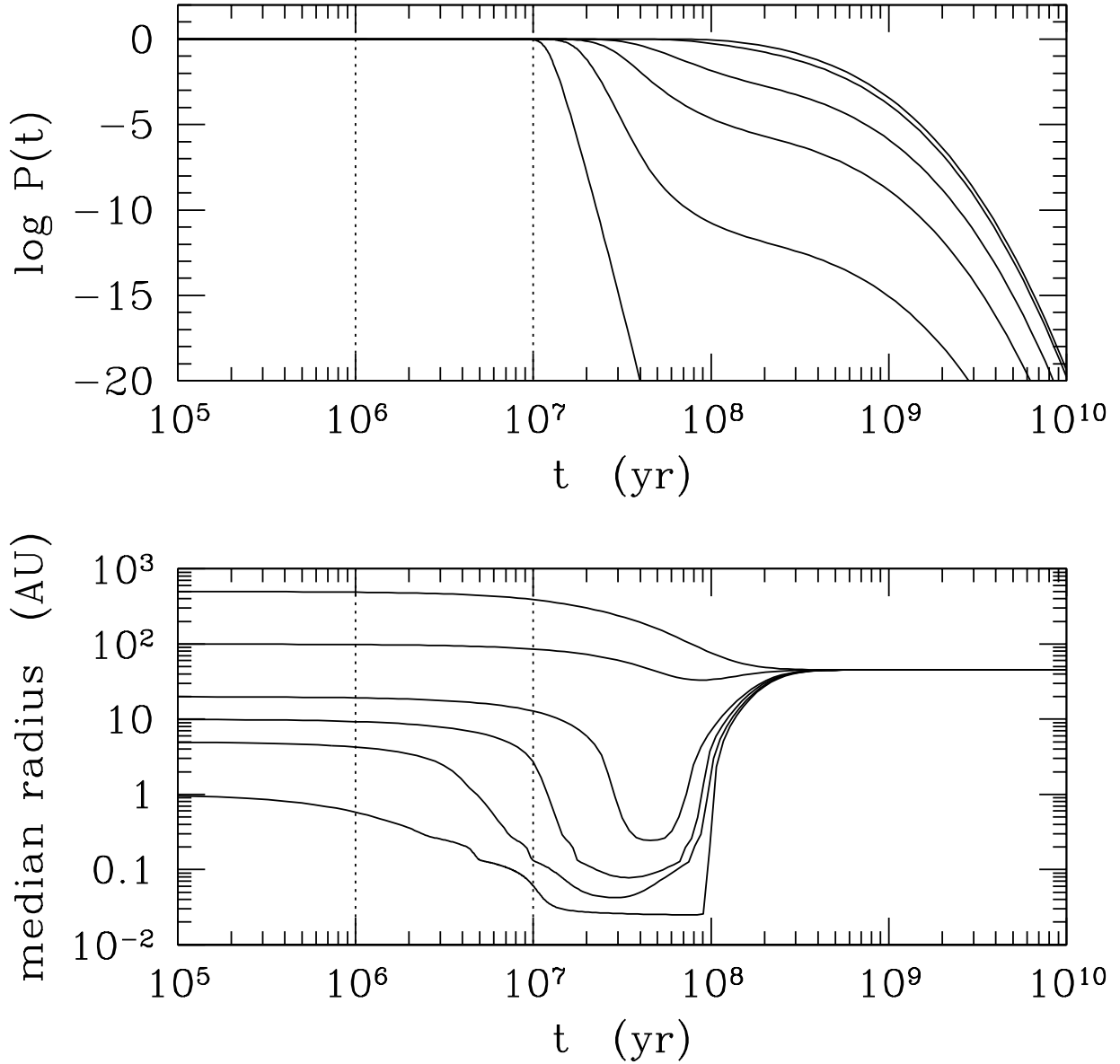


Fig. 5.— Evolution of the survival probability, P (upper panel), and of the median radius of surviving planets (lower panel) for Earth-mass planets formed in a localized burst at $t = 0$ in the T-Tauri alpha-disk model (with $\alpha = 0.02$). Torque fluctuations were normalized to $\epsilon = 0.5$. In each panel, the six solid lines correspond to planets formed at $r_S = 500, 100, 20, 10, 5$ and 1 AU (from top to bottom). Vertical dotted lines bracket typical protoplanetary disk lifetimes. As before, a declining fraction of planets survives for long times but in these models the median radii reach an asymptotic value at which the sum of the secular and diffusive contributions to advection is minimized. The advection of most planets at intermediate times is clearly visible in the median radius evolution.

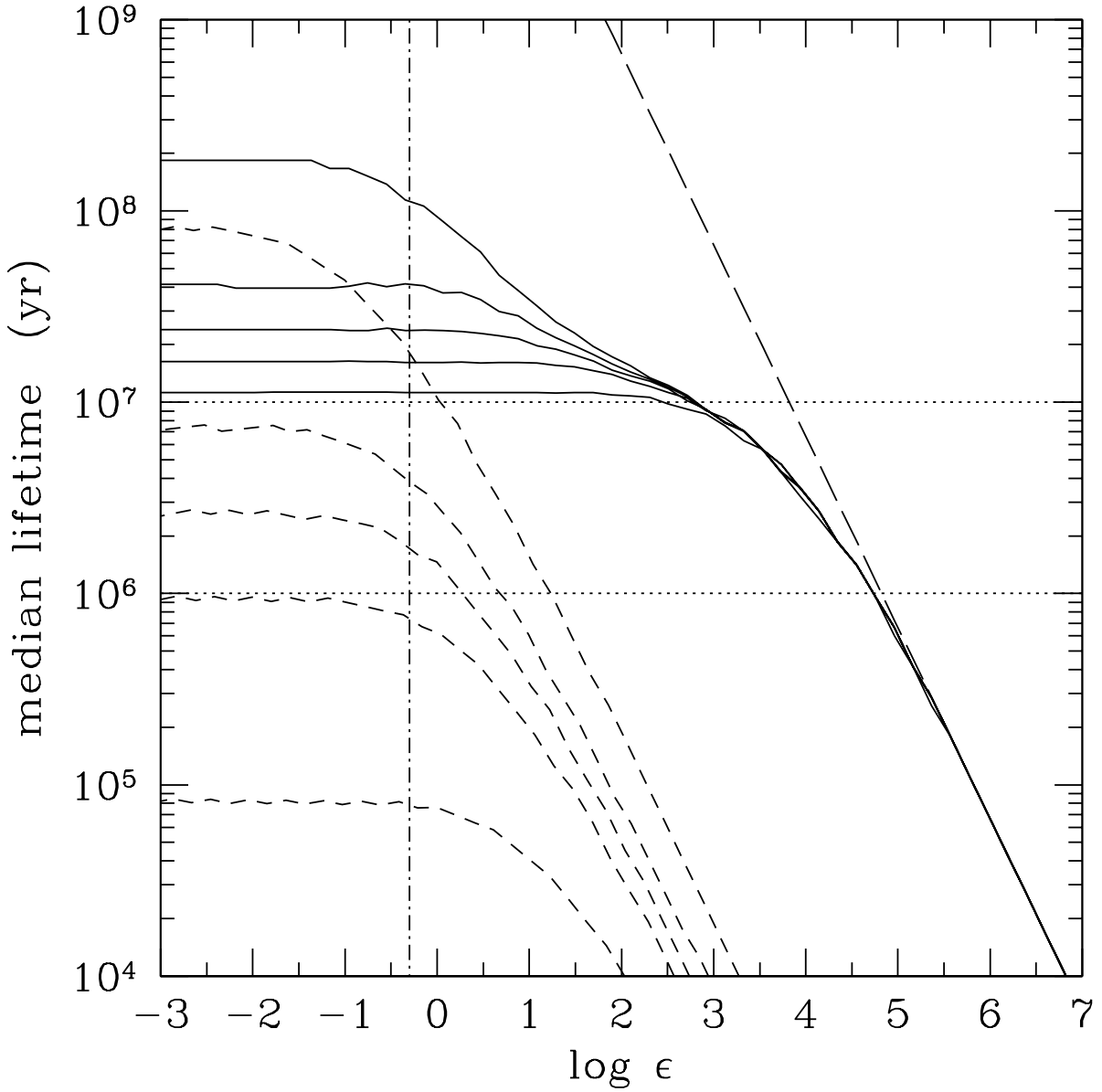


Fig. 6.— Median lifetimes as a function of torque fluctuation normalization, ϵ , for Earth-mass planets formed in a burst at radii $r_S = 100, 20, 10, 5$ and 1 AU (from top to bottom) in the MMSN (dashed lines) and in the alpha-disk model (solid lines; $\alpha = 0.02$). The vertical dash-dotted line corresponds to our fiducial calibration of torque fluctuations ($\epsilon = 0.5$). Horizontal dotted lines bracket typical protoplanetary disk lifetimes. The long-dashed line indicates the median lifetimes expected in the alpha-disk model in the limit of negligible mean torque. Diffusion is unimportant at low ϵ values, but it can significantly reduce the median lifetimes of planets formed at any radius for large enough ϵ values.

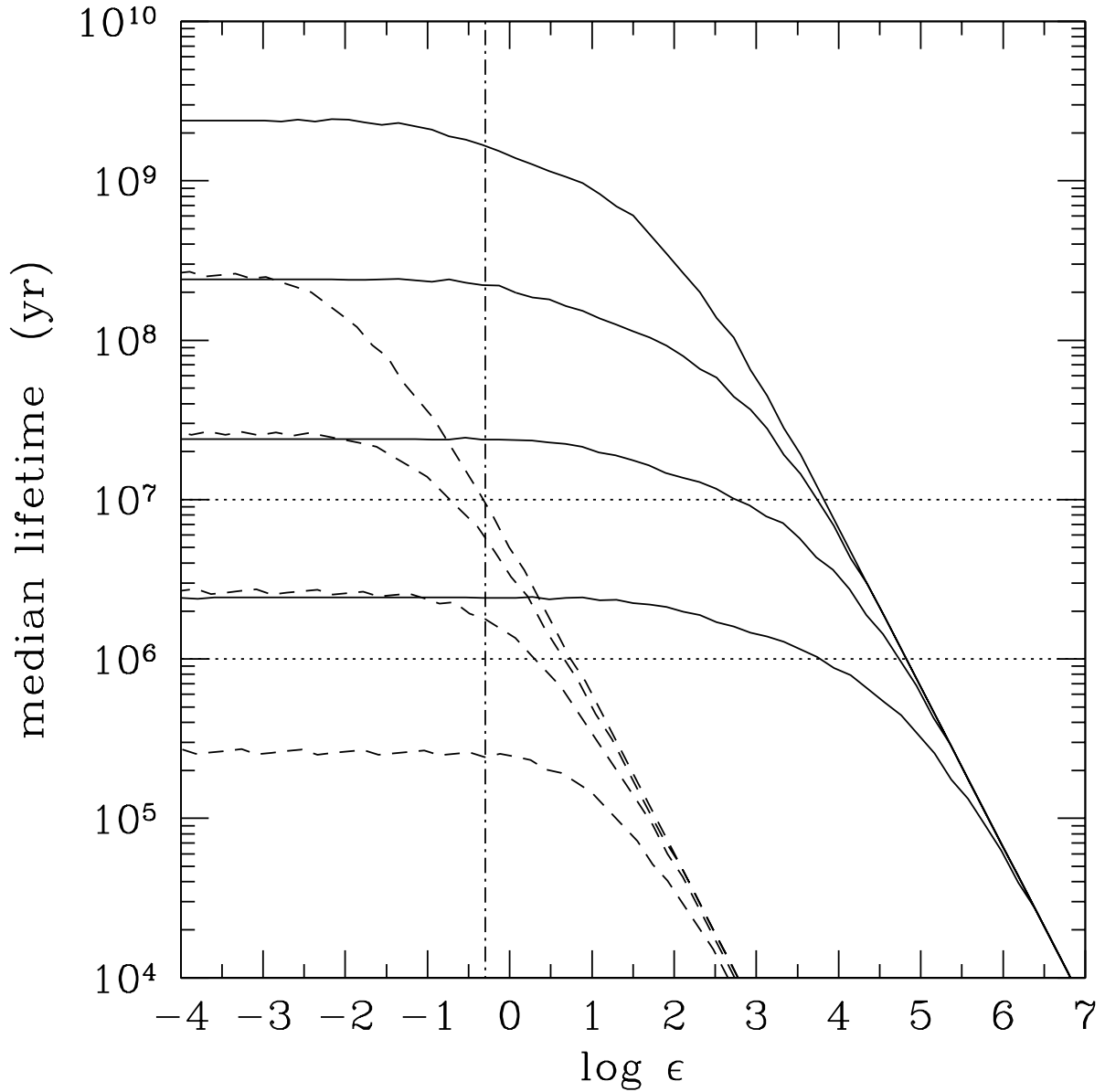


Fig. 7.— Median lifetimes as a function of torque fluctuation normalization, ϵ , for planets of various masses all formed in a burst at $r_S = 10$ AU in the MMSN (dashed lines) and in the alpha-disk model (solid lines; $\alpha = 0.02$). The various curves correspond to planets of mass $M_p = 0.01, 0.1, 1$ and $10M_{\oplus}$ (from top to bottom). The vertical dash-dotted line corresponds to our fiducial calibration of torque fluctuations ($\epsilon = 0.5$). Horizontal dotted lines bracket typical protoplanetary disk lifetimes. Diffusion is unimportant at low ϵ values, but it can significantly reduce the median lifetimes of planets of any mass ($\lesssim 10M_{\oplus}$) for large enough ϵ values.